

Localized eigenvectors on metric graphs

H. Kravitz ^{*1}, M. Brio ^{†2} and J.-G. Caputo ^{‡3}

¹Fariborz Maseeh Department of Mathematics and Statistics, Portland State University, 1825 SW Broadway, Portland, OR 97201, United States of America

²Department of Mathematics, University of Arizona, 617 North Santa Rita Avenue, Tucson Arizona, 85721, United States of America

³Laboratoire de Mathématiques, INSA de Rouen Normandie, Avenue de l'Université, Saint-Etienne du Rouvray, 76801, France

Abstract

Using our previously published algorithm, we analyze the eigenvectors of the generalized Laplacian for two metric graphs occurring in practical applications. As expected, localization of an eigenvector is rare and the network should be tuned to observe exactly localized eigenvectors. We derive the resonance conditions to obtain localized eigenvectors for various geometric configurations and their combinations to form more complicated resonant structures. These localized eigenvectors suggest a new localization indicator based on the L_2 norm. They also can be excited, even with leaky boundary conditions, as shown by the numerical solution of the time-dependent wave equation on the metric graph. Finally, the study suggests practical ways to make resonating systems based on metric graphs.

Keywords: partial differential equations, metric graphs, localization

1 Introduction

Partial differential equations (PDEs) on networks arise in many physical applications such as gas and water networks [1, 2], electromechanical waves in a transmission grid [3], air traffic control [4], microwave networks [5] and random nanofiber lasers [6, 7] to name a few. In many cases, the problem can be linearized. Then separation of variables yields a Helmholtz (or Schrödinger)

*hkravitz@pdx.edu

†brio@math.arizona.edu

‡jean-guy.caputo@insa-rouen.fr

problem on the network. The associated eigenvalues and eigenvectors play a fundamental role in the theoretical analysis of the networks [8] and the practical applications.

The underlying mathematical model consists of a metric graph: a finite set of vertices connected by arcs (oriented edges) on which a metric is assigned. Different coupling conditions can be implemented at the vertices. The simplest assumes continuity of the field and zero total gradient at the vertices (Kirchhoff's law). The standard one-dimensional Laplacian together with these boundary conditions results in a generalized Laplacian and associated Helmholtz eigenvalue problem. It can be shown that with these coupling conditions (continuity and Kirchhoff's law) the operator is self-adjoint [8], yielding real eigenvalues and orthogonal eigenvectors. The eigenvectors form a complete basis of the appropriate set of square integrable functions on the graph. This spectral framework plays a key role in linear PDEs. We review and apply it in the present article.

Combinatorial or discrete graphs bear some similarities to metric graphs. For these graphs, edges only describe connections between vertices. For undirected graphs, both the adjacency matrix and the graph Laplacian are symmetric—they have real eigenvalues, and the eigenvectors can be chosen orthogonal. Some eigenvectors have non zero components on just a few vertices, they are *localized* and this localization affects transport properties [9]. In a recent article [10] we showed that the Laplacian eigenvectors of chains connected to complete graphs are localized in the complete graph regions where connectivity is high. These results were also found in the systematic study by Hata and Nakao [11] where they analyzed graphs with random degree distributions. The localization of eigenvectors found here is purely topological because the Laplacian has equal weights. Random weights introduce additional possibilities for localizing the eigenvectors, see the pioneering 1958 study by Anderson [12] of a Schrödinger matrix equation with random diagonal and off-diagonal elements and the very large literature that followed it.

In contrast, the localization of eigenvectors on arcs of random metric quantum graphs has only been studied in a handful of articles and many of these assume non standard interface conditions at the vertices. For the standard conditions, Schanz and Kottos [23] established conditions for localized eigenvectors in polygons. They use a scattering theory formalism because they were interested in problems of quantum chaos. In another interesting study, Gnutzman, Schanz and Smilansky [22], using similar tools, established that localized eigenvectors cannot exist in trees and recovered the conditions for localization in polygons. Because of the formalism used and despite their importance, these results are not so well known in the engineering community studying networks.

To study these practical network problems, we introduced recently a systematic procedure to compute eigenvalues and eigenvectors of arbitrary order for general metric graphs [18]. In the present article, we use this method to analyze two metric graphs occurring in engineering applications and examine the occurrence of localized eigenvectors. Using simple arguments, we examined the

conditions to observe exactly localized eigenvectors, starting from the simplest. We found the precise resonance conditions on the lengths and the eigenvalues for several geometric configurations such as a cycle with two edges and a polygon; we recover some results of [23], [22] and find new ones. In particular, we show how these localized eigenvectors can be connected to form a larger localized eigenvector; this can be important for resonator applications. These results on localized eigenvectors prompted us to define a localization criterion giving the number of edges involved in a localized eigenvector. Finally, the numerical solution of the wave equation on the metric graph reveals how these localized eigenvectors can be excited from a broadband initial condition.

The article is organized as follows. The statement of the problem, A brief review of the spectral properties of metric quantum graphs and of our computational algorithm are given in Section 2. There we also compute numerically and characterize the eigenvectors of two metric graphs. Section 3 lists exact resonant conditions to obtain localized eigenvectors in various geometric configurations. The localization criteria are discussed in Section 4. We also show how the solution of the wave equation with a leaky boundary converges to a localized eigenvector. Section 5 concludes the article.

2 Spectral theory for metric graphs

We first recall the spectral theory formalism for completeness. We will then illustrate it on two examples from engineering applications.

Consider a finite metric graph with n vertices connected by m arcs (oriented edges) of length l_j , $j = 1 : m$. Each edge is parameterized by its length x from the origin vertex $x = 0$ to the terminal vertex $x = l_j$. We recall the definition of the *degree* of a vertex: the number of edges connected to it.

On this graph, we define the vector component wave equation

$$U_{tt} - \tilde{\Delta}U = 0, \quad (1)$$

where $U \equiv (u_1, u_2, \dots, u_m)^T$. Each component satisfies the one-dimensional wave equation inside the respective arc,

$$u_{jtt} - u_{jxx} = 0, \quad j = 1, 2, \dots, m \quad (2)$$

In addition, the solution should be continuous at the vertices and also satisfy the Kirchhoff flux conditions at each vertex of degree d

$$\sum_{j=1}^d u_{jx} = 0, \quad (3)$$

where u_{jx} represent the outgoing fluxes for arc j emanating from the vertex.

Consider equation (1). Since the problem is linear, we can separate time and space and assume a harmonic solution $U(x, t) = e^{ikt} V(x)$. We then get a Helmholtz or Schrödinger eigenproblem for V on the graph

$$-\tilde{\Delta}V = k^2V, \quad (4)$$

and where $\tilde{\Delta}$ is the generalized Laplacian, i.e. the standard Laplacian on the arcs together with the coupling conditions at the vertices. Note that we exclude all degree two vertices since due to continuity and the Kirchhoff condition, two edges sharing such a vertex can be merged into a single edge—see [19].

The generalized eigenvalue problem (4) admits an inner product obtained from the standard inner product on L_2 space—see [8]. We have

$$\langle f, g \rangle \equiv \sum_{\text{arc } j} \langle f_j, g_j \rangle, \quad \langle f_j, g_j \rangle = \int_0^{l_j} f_j(x)g_j(x)dx. \quad (5)$$

A solution in terms of Fourier harmonics on each branch j of length l_j is

$$v_j(x) = A_j \sin kx + B_j \cos kx. \quad (6)$$

Writing down the coupling conditions at each vertex, one obtains a homogeneous linear system whose k -dependent matrix is singular at the eigenvalues.

Using solution (6) on each arc with unknown coefficients A_j and B_j , the coupling conditions at each vertex yield the homogeneous system

$$M(k)X = 0, \quad (7)$$

of $2m$ equations for the vector of $2m$ unknown arc amplitudes

$$X = (A_1, B_1, A_2, B_2, \dots, A_m, B_m)^T.$$

The matrix $M(k)$ is singular at the eigenvalues $-k^2$. We call these k -values resonant frequencies. A practical and robust computational algorithm for the computation of these eigenvalues and eigenvectors was proposed and studied in [18].

For each resonant frequency k_q , the eigenvectors V^q span the null space of the matrix $M(k_q)$. They can then be written as

$$V^q = \begin{pmatrix} A_1^q \sin k_q x + B_1^q \cos k_q x \\ A_2^q \sin k_q x + B_2^q \cos k_q x \\ \dots \\ A_m^q \sin k_q x + B_m^q \cos k_q x \end{pmatrix} \quad (8)$$

They can be normalized using the scalar product defined above. We have

$$\|V^q\|^2 = \langle V^q, V^q \rangle = \sum_{j=1}^m \langle V_j^q, V_j^q \rangle, \quad (9)$$

where

$$V_j^q = A_j^q \sin k_q x + B_j^q \cos k_q x, \quad (10)$$

and $\langle V_j^q, V_j^q \rangle$ is the standard scalar product on $L_2([0, l_j])$. This defines a broken L_2 norm or graph norm. The scalar product $\langle V_j^q, V_j^q \rangle$ can be computed explicitly

$$\begin{aligned} \langle V_j^q, V_j^q \rangle &= \left(A_j^{q2} + B_j^{q2} \right) \frac{l_j}{2} \\ &+ \frac{\sin 2k_q l_j}{4k_q} \left(-A_j^{q2} + B_j^{q2} \right) + A_j^q B_j^q \frac{1 - \cos 2k_q l_j}{2k_q}. \end{aligned} \quad (11)$$

It has been shown that, for the standard coupling conditions used here (continuity and Kirchhoff's condition), the eigenvectors V^i form a complete orthogonal basis of the Cartesian product $L_2([0, l_1]) \times L_2([0, l_2]) \cdots \times L_2([0, l_m])$ —see [8].

Once the eigenvalue problem is solved, one can proceed with the spectral solution of the time-dependent problem, exactly as for the one-dimensional wave equation on an interval. For that, expand the solution of the wave equation on the graph (1) using the eigenvectors,

$$U(x, t) = \sum_{q=1}^{\infty} a_q(t) V^q, \quad (12)$$

and obtain a simplified description of the dynamics in terms of the amplitudes a_q .

2.1 Localized eigenvectors : two numerical examples

Like the eigenvectors of the discrete Laplacian, eigenvectors of the generalized Laplacian on a network can be localized in the following sense.

Definition 2.1 (Localized eigenvector) *An eigenvector V^i of the generalized Laplacian operator with the standard coupling conditions is localized if its components V_j^i (see (10)) satisfy $V_j^i \neq 0$ for a finite number of edges j and $V_j^i = 0$ for the rest.*

Such a localized eigenvector plays an important role in the dynamics of the wave equation.

We consider two graphs with no symmetries and arbitrary edges to illustrate how frequently localized eigenvectors appear. To identify these eigenvectors, we compute the L_2 norm ratio

$$e_q(j) \equiv \frac{\langle V_j^q, V_j^q \rangle}{\langle V^q, V^q \rangle} \quad (13)$$

for each edge $j = 1, 2, \dots, m$.

2.2 Graph G14

We introduce the 14 edge graph—see Fig. 1. It was adapted from IEEE case 14 [21] by eliminating the degree two vertices. Such a metric graph can be used to model how electromechanical waves propagate in an electrical grid [3]. A localized eigenvector in this context would correspond to an accumulation of energy on just a few equipments and this could cause their failure.

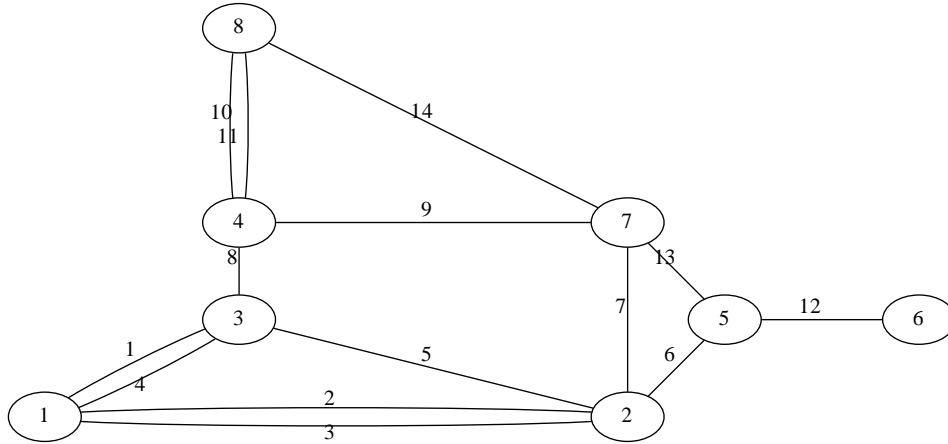


Figure 1: The 14 vertex metric graph G14

The lengths $l_i, i = 1, \dots, m = 14$ are given in Table 1.

l_1	l_2	l_3	l_4	l_5	l_6	l_7
11.91371443	7.08276253	6	2.236067977	4.123105626	1.414213562	2
l_8	l_9	l_{10}	l_{11}	l_{12}	l_{13}	l_{14}
1	4.7169892	4.472135955	2	2	1.414213562	4.472135955

Table 1: The lengths l_i for the graph G14 .

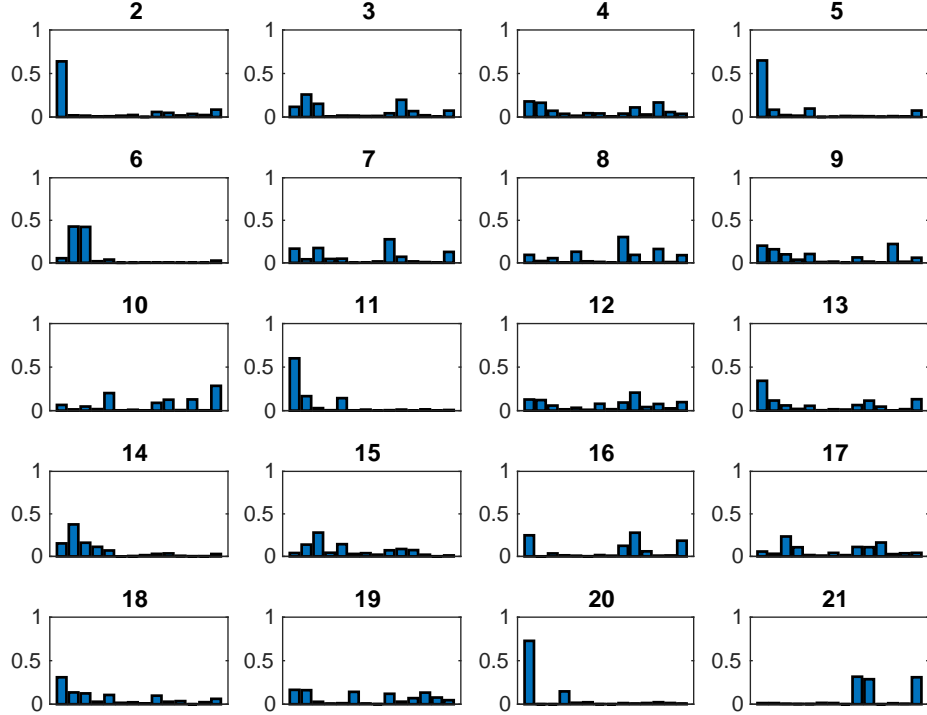


Figure 2: Histograms of the L_2 norm ratio $e_q(j)$ (13) for $q = 2, \dots, 21$ from left to right and top to bottom for the G14 graph.

Fig. 2 presents the histograms of the L_2 norm ratio $e_q(j)$ for eigenvectors V^q , $q = 2, \dots, 21$ for the G14 graph. Note that $q = 2, 5, 6, 11, 20$ and 21 correspond to eigenvectors where $e_q(j) \geq 0.5$ for one or two edges j and $e_q(j) < 0.05$ for the other edges. In Fig. 3 we present the approximately localized eigenvectors corresponding to $q = 2, 5, 6, 11, 20$ and 21 . For a given eigenvector V^q , we present for each edge j the quantity $e_q(j)$.

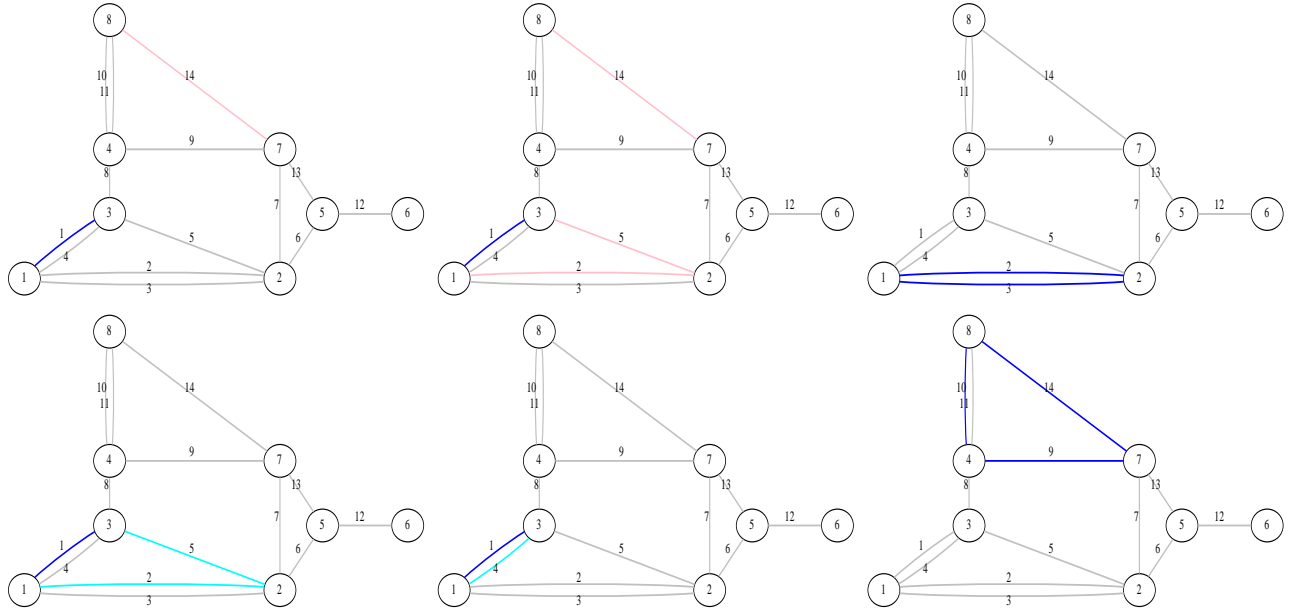


Figure 3: Approximately localized eigenvectors V^q for $q = 2, 5, 6, 11, 20$ and 21 . We present for each arc j the quantity $e_q(j)$ with the color code $e_q(j) < 0.06$ (grey), $0.06 < e_q(j) < 0.12$ (pink), $0.12 < e_q(j) < 0.2$ (cyan) and $0.2 < e_q(j)$ (blue). The values of k_q are given in the table below.

The values of k_q are presented in Table 2 below.

0.2347645148	0.4657835674	0.480197067
0.8078723081	1.3322287766	1.379308786

Table 2: The values of k_q shown in Fig. 3.

2.3 Buffon graph

The second example we present comes from a study by Gaio et al [6] suggesting that lasers can be produced by fusing randomly placed nanometric optical waveguides. The resulting graph appears as a series of scattered needles. Such a Buffon's needle graph with 165 arcs and 104 vertices is shown in Fig. 4.

In Gaio's study, the fibers are active so that they would amplify the field. The lasing effect would come from a balance between this amplification and damping. In addition, there would be transparent conditions at the boundaries so that any out-going radiation would be lost. Then, a laser effect would occur on the localized eigenvectors of the Laplacian and only on those because the extended eigenvectors would be damped due to the boundary conditions.

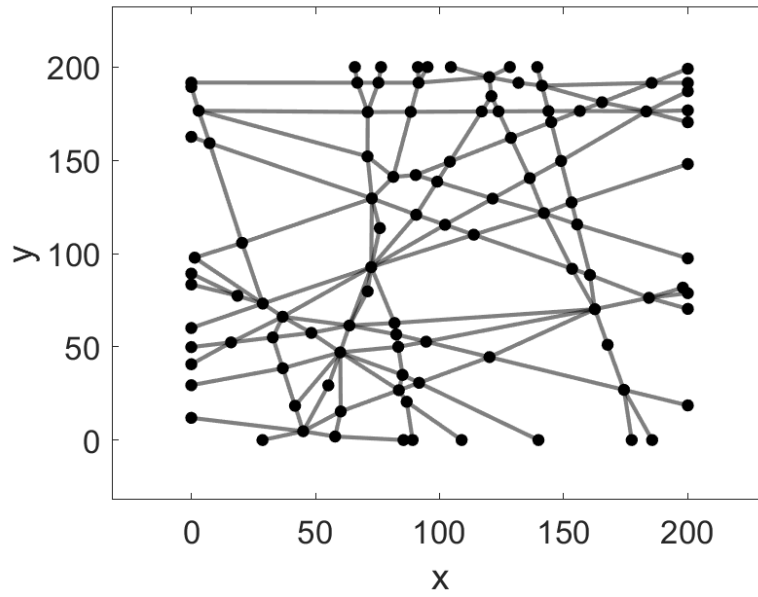


Figure 4: A Buffon's needle graph with $m = 104$ vertices and $m = 165$ arcs.

Fig. 5 presents the histograms of the L_2 norm ratio $e_q(j)$ for eigenvectors V^q , $q = 2, \dots, 21$ for the Buffon graph of Fig. 4.

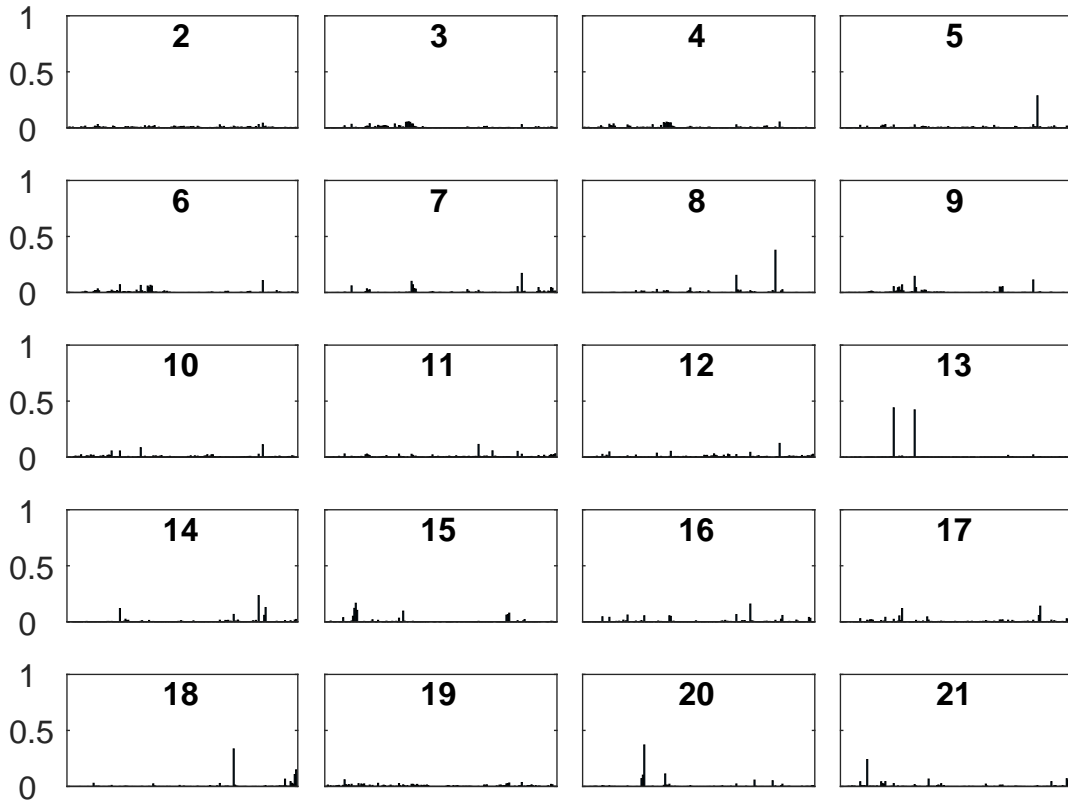


Figure 5: Histograms of the L_2 norm ratio $e_q(j)$ (13) for $q = 2, \dots, 21$ from left to right and top to bottom for the Buffon graph.

The vectors V^q for $q = 5, 8, 13, 18, 20$ and 21 are approximately localized. They are plotted below.

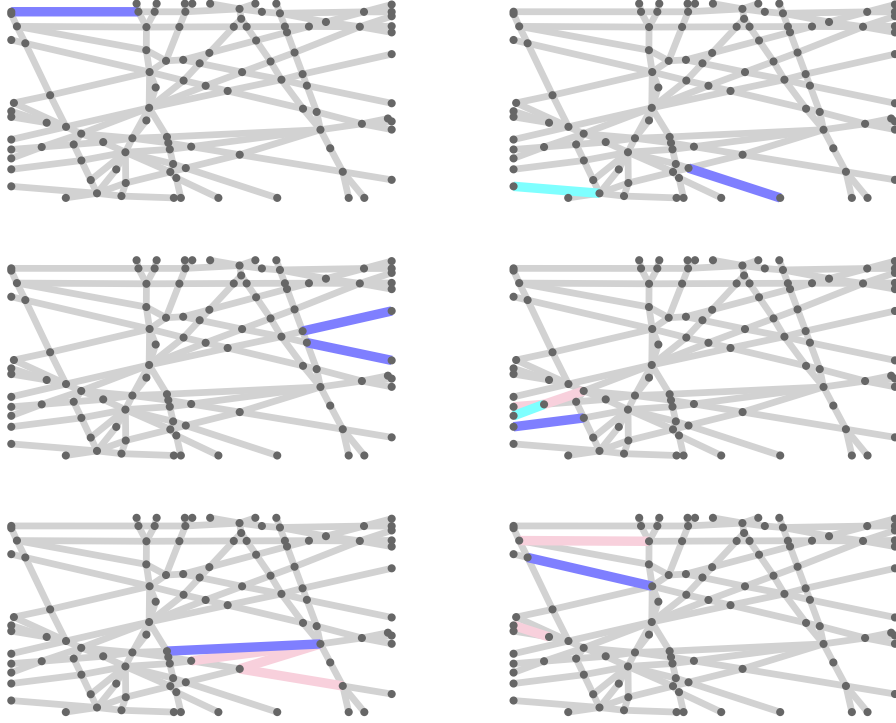


Figure 6: Plots of the localized eigenvectors V^q for $q = 5, 8, 13, 18, 20$ and 21 . The color code is $e_q(j) < 0.06$ (grey), $0.06 < e_q(j) < 0.12$ (pink), $0.12 < e_q(j) < 0.2$ (cyan) and $0.2 < e_q(j)$ (blue).

The corresponding values of k_q are shown in Table 3

0.016866927	0.022719737	0.029337666
0.034764362	0.036236231	0.036802227

Table 3: The values of k_q shown in Fig. 6.

The results of this section illustrate that for arbitrary metric graphs, approximately localized eigenvectors occur, in particular we observed them for large k . However, this localization is not exact. This is a known result, see the statement "there are no perfect scars for generic graphs" by Schanz and Kotos [23]. For the laser application [6], a lasing phenomenon is therefore unlikely to appear in a random arrangement of nanometric waveguides.

For exactly localized eigenvectors to exist, we need a precise arrangement of the lengths of the arcs involved. We give these resonance conditions in the next

section.

3 Exactly localized eigenvectors

We examine configurations that lead to *exactly localized eigenvectors* following the definition (2.1). In the rest of this section we drop the adjective *exactly*. We find that localized eigenvectors exist on two connected leaves, as a 1-2 state in a pumpkin, as a triangle 1-2-3 and a quadrilateral 1-2-3-4—see Table 5. The analysis also enables us to rule out single arc, leaf, two connected arcs and degree three vertex localized eigenvectors—see Table 6.

We show the computations in detail for the 1-2-3 triangle. Calculations for the other examples are given in the appendix.

3.1 A localized eigenvector, the Triangle 1-2-3

Consider the configuration of Fig. 7 where a triangle of edges l_1, l_2, l_3 is embedded in a graph.

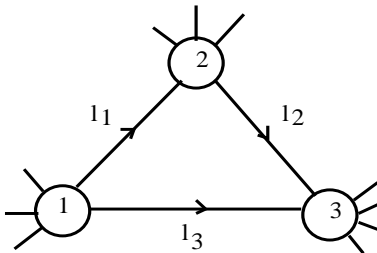


Figure 7: A triangle 1-2-3 embedded in a graph.

We have the following theorem.

Theorem 3.1 *A localized eigenvector exists on a triangle of edges l_1, l_2, l_3 embedded in a graph if there exists three integers n_1, n_2, n_3 such that*

$$\frac{l_1}{n_1} = \frac{l_2}{n_2} = \frac{l_3}{n_3}$$

and $n_1 + n_2 + n_3$ is even.

The eigenvalue is $-\left(\frac{n_1\pi}{l_1}\right)^2$ and the eigenvector is

$$V = \sin kx(1, (-1)^{n_1}, -1)^T$$

Proof. On each edge j , we have $V_j = A_j \sin kx + B_j \sin kx$. To have a localized eigenvector, we need that at each vertex $V = 0$ and to balance the fluxes. These conditions are

$$\begin{aligned} V_1(0) &= V_3(0) = 0, \\ V_{1x}(0) + V_{3x}(0) &= 0, \\ V_1(l_1) &= V_2(0) = 0, \\ V_{1x}(l_1) - V_{2x}(0) &= 0, \\ V_3(l_3) &= V_2(l_2) = 0, \\ V_{3x}(l_3) + V_{2x}(l_2) &= 0, \end{aligned}$$

yielding

$$\begin{aligned} kl_1 &= n_1\pi, \quad kl_2 = n_2\pi, \quad kl_3 = n_3\pi, \\ \frac{l_1}{l_2} &= \frac{n_1}{n_2}, \quad \frac{l_1}{l_3} = \frac{n_1}{n_3}, \\ B_1 &= B_2 = B_3 = 0, \\ A_3 &= -A_1, \\ A_2 &= A_1 c_1, \\ A_2 c_2 + A_3 c_3 &= 0, \end{aligned}$$

where n_1, n_2, n_3 are integers and $c_1 = \cos kl_1, \dots$. Using the last relation, we get the condition

$$(-1)^{n_1+n_2} = (-1)^{n_3}, \quad (14)$$

so that $n_1 + n_2 + n_3$ is even. To summarize, we have a triangle eigenvector if there exists four integers n_0, n_1, n_2, n_3 such that

$$\frac{l_1}{n_1} = \frac{l_2}{n_2} = \frac{l_3}{n_3}, \quad (15)$$

$$n_1 + n_2 + n_3 = 2n_0. \quad (16)$$

The eigenvector is

$$V = \sin kx(1, (-1)^{n_1}, -1)^T$$

□

Fig. 8 shows such a state for $k = 1$ in the G14 graph, with $l_6 = 2\pi$, $l_7 = 3\pi$ and $l_{13} = 7\pi$.

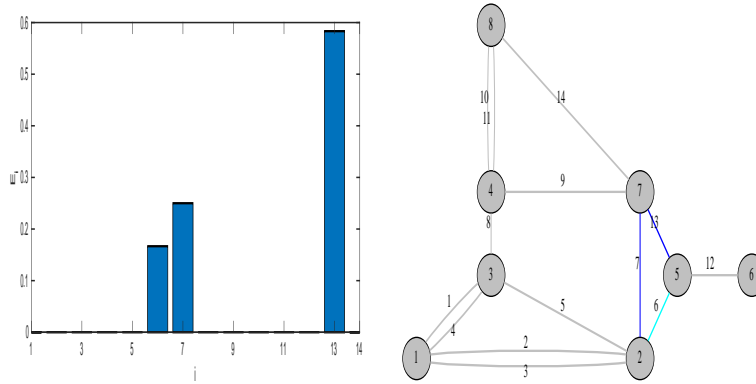


Figure 8: A triangle 1-2-3 "embedded" in a graph. The active arcs are 6,7 and 13.

Here, we recover in a simple way the conditions obtained by Gnutzmann et al [22] using scattering theory arguments. Similarly, we can obtain a localized eigenvector on a quadrilateral or any polygon. Fig. 9 shows such an exactly localized eigenvector on the quadrilateral 5-7-8-9 for the G14 graph where we chose

$$l_5 = 2\pi, l_7 = 3\pi, l_8 = 5\pi, l_9 = 6\pi.$$

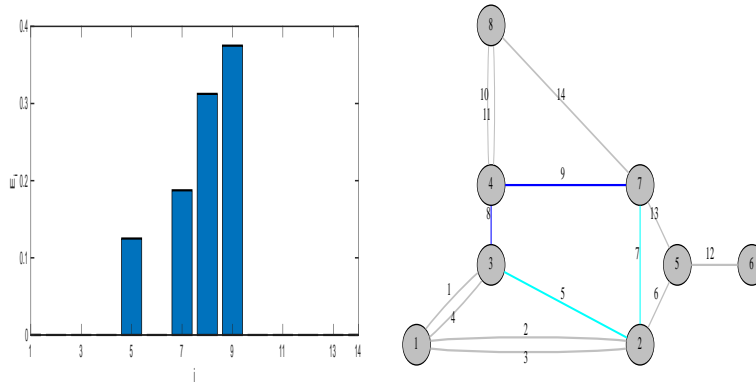


Figure 9: A quadrilateral 1-2-3-4 embedded in a graph. The active arcs are 5,7,8 and 9.

3.2 1-2 localized eigenvector on a pumpkin subgraph

We present here a localized eigenvector that is new to the best of our knowledge. It is a 1-2 or more resonance in a pumpkin subgraph. Pumpkin graphs were studied in detail by Berkolaiko [20] who introduced this terminology.

Definition 3.2 An m -pumpkin graph consists of two vertices and m parallel edges of possibly different lengths running between them.

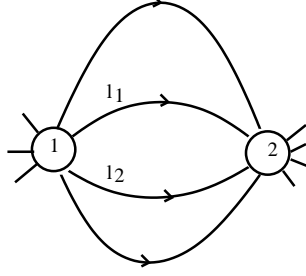


Figure 10: A 2-pumpkin 1-2 embedded in a graph.

Consider the configuration of Fig. 10 where a pumpkin is embedded in a graph. For certain edge lengths l_1, l_2 , there exists a localized eigenvector on these two edges.

Theorem 3.3 A localized eigenvector exists on a pumpkin subgraph of a metric graph with at least two edges l_1, l_2 if there are two integers n_1, n_2 of same parity such that

$$\frac{l_1}{n_1} = \frac{l_2}{n_2}.$$

Proof. As for the triangle, we want V to be zero at the vertices and to balance the flux, then

$$\begin{aligned} V_1(0) &= V_2(0) = 0, \\ V_1(l_1) &= V_2(l_2) = 0, \\ V_{1x}(0) + V_{2x}(0) &= 0, \\ V_{1x}(l_1) + V_{2x}(l_2) &= 0. \end{aligned}$$

This yields the system of equations

$$\begin{aligned} B_1 &= B_2 = 0, \\ A_1 \sin kl_1 &= A_2 \sin kl_2 = 0, \\ A_1 + A_2 &= 0, \\ A_1 \cos kl_1 + A_2 \cos kl_2 &= 0. \end{aligned}$$

We then obtain

$$\sin kl_1 = 0, \quad \sin kl_2 = 0,$$

so that

$$kl_1 = n_1\pi, \quad kl_2 = n_2\pi,$$

where n_1, n_2 are integers. Then $\cos kl_1 = (-1)^{n_1}$, $\cos kl_2 = (-1)^{n_2}$. A non-trivial solution A_1, A_2 exists only if $\cos kl_1 = \cos kl_2$ so that n_1 and n_2 have the same parity. The condition on the lengths is then

$$\frac{l_1}{n_1} = \frac{l_2}{n_2}, \quad (17)$$

where n_1, n_2 are integers of same parity. □

To illustrate this localized eigenvector, consider the graph shown in Fig. 11.

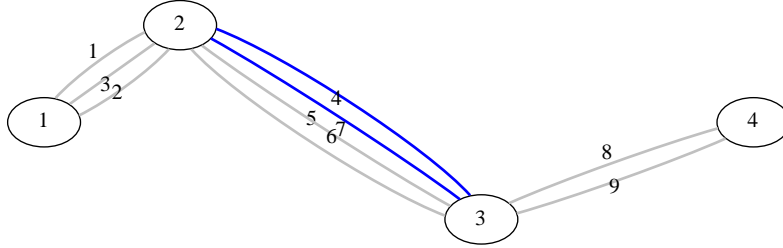


Figure 11: A graph showing a localized 1-2 pumpkin eigenvector.

The lengths are given in Table 4, where the arcs 4 and 7 satisfy the resonance condition (17). The localized eigenvector on arcs 4 and 7 is shown with the color code $e_q(j) < 0.06$ (grey), $0.06 < e_q(j) < 0.12$ (pink), $0.12 < e_q(j) < 0.2$ (cyan) and $0.2 < e_q(j)$ (blue).

l_1 2.236067977	l_2 1.414213562	l_3 1.732050807	l_4 π	l_5 11π
l_6 5.167771571	l_7 9.424777960	l_8 3.605551275	l_9 5.693156148	

Table 4: The lengths l_i for the graph shown in Fig. 11.

Similarly, one can have a localized eigenvector on a 3-pumpkin. The derivation is similar to the 2-pumpkin. We obtain the conditions

$$A_1 + A_2 + A_3 = 0,$$

$$\frac{l_1}{n_1} = \frac{l_2}{n_2} = \frac{l_3}{n_3}$$

where n_1, n_2 and n_3 are integers of the same parity. Note that the eigenspace has dimension 2.

To conclude this section, Table 5 gives four configurations giving localized eigenvectors.

2 connected leaves	1-2 eigenvector in a pumpkin	triangle 1-2-3	quadrilateral 1-2-3-4
$\frac{l_1}{n_1} = \frac{l_2}{n_2}$ n_1, n_2 odd integers	$\frac{l_1}{n_1} = \frac{l_2}{n_2}$ n_1, n_2 integers same parity	$\frac{l_1}{n_1} = \frac{l_2}{n_2} = \frac{l_3}{n_3}$ n_1, n_2, n_3 integers $n_1 + n_2 + n_3$ even	$\frac{l_1}{n_1} = \frac{l_2}{n_2} = \frac{l_3}{n_3} = \frac{l_4}{n_4}$ n_1, n_2, n_3, n_4 integers $n_1 + n_2 + n_3 + n_4$ even

Table 5: Four configurations giving localized eigenvectors and conditions for the lengths of the arcs.

Connecting eigenvectors

Two elementary graphs corresponding to localized eigenvectors for the same eigenvalue can be connected to yield a composite graph for the same eigenvalue. We have the following.

Theorem 3.4 *Consider two elementary graphs G_1, G_2 corresponding to localized eigenvectors of the generalized Laplacian for the same eigenvalue. Then, the composite graph obtained by joining a vertex from G_1 to a vertex from G_2 has the same eigenvalue.*

Proof.

The proof is elementary. The eigenvector components V_j^1, V_k^2 are zero at each vertex of G_1 and G_2 respectively so that the zero condition is satisfied for both subgraphs.

Since the fluxes are balanced separately for G_1 and G_2 , they will be balanced for the composite graph. This shows that the union of the eigenvectors V^1, V^2 is a localized eigenvector for the composite graph. \square

A consequence of this result is that the composite graph can be a subgraph of a large graph and have the same eigenvalue as long as there are no "external" edges i.e. not belonging to G_1 and G_2 .

3.3 No single arc eigenvector

The methodology given above also allows us to rule out geometric situations where no localized eigenvector exists. As an example, consider a single arc.

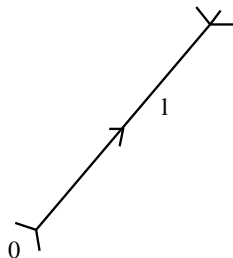


Figure 12: An arc embedded in a graph.

We have the following theorem

Theorem 3.5 *A localized eigenvector of the generalized Laplacian cannot exist on an arc embedded in a metric graph.*

Proof. To show this, consider Fig. 12. The localization conditions for the solution

$$V = A \sin kx + B \cos kx$$

are

$$V(0) = V(l) = 0, \quad V(0)_x = V_x(l) = 0$$

This yields $A = B = 0$ so that a localized eigenvector cannot exist. \square

This is a known result [23].

Table 6 gives four configurations where localized eigenvectors do not exist. Details of the calculations are given in the appendix.

single arc	leaf eigenvector	two connected arcs	degree 3 vertex eigenvector
---------------	---------------------	-----------------------	--------------------------------

Table 6: Four configurations where a localized eigenvector cannot exist.

4 Discussion: localization criterion and excitation

The histograms of the energy components $\langle V_j^q, V_j^q \rangle$ of the localized eigenvectors show differences despite the fact that the A coefficients are the same. This imbalance is due to the different lengths of the arcs j because $\langle V_j^q, V_j^q \rangle$ scales like l_j —see (11).

To correct the imbalance, we use equation (13) and rescale $\langle V_j^q, V_j^q \rangle$ by l_j . For that we introduce the localization criterion for an eigenvector V^q as

$$\mathcal{L}_q = \max_j E_j^q, \quad (18)$$

where

$$E_j^q \equiv \frac{\langle V_j^q, V_j^q \rangle}{l_j \sum_k \frac{\langle V_k^q, V_k^q \rangle}{l_k}} \quad (19)$$

where we use the graph norm (9).

The calculations of the previous section for the two leaf, the triangle and the quadrilateral localized eigenvectors can be used to exactly compute \mathcal{L}_q . The results are shown in Table 7. To illustrate the usefulness of E_j^q , observe that the histograms presented in the left panels of Figs. 8 and 9 will have all the same amplitude if E_j^q is used instead of $e_q(j)$ (13); the amplitudes will be 1/3 and 1/4 respectively, see Table 7. This shows that $1/\mathcal{L}_q$ gives the number of active arcs. The analysis of the previous section shows that an eigenvector is localized on at least two arcs with equal amplitudes $A_1 = A_2$. Then a general upper bound is

$$\mathcal{L}_q \leq 0.5$$

The quantity E_j^q is the energy density of edge j . When applied to arbitrary metric graphs such as the G14, it indicates the regions of the graph that are most active.

In contrast, the standard localization criterion

$$IPR_q = \frac{\sum_{j=1}^m \int_0^{l_j} |V_j^q|^4 dx}{(\sum_{j=1}^m \int_0^{l_j} |V_j^q|^2 dx)^2}, \quad (20)$$

used for example by Gaio [6] does not give such precise information on the active arcs, as it is not based on localized eigenvectors. Table 7 shows the IPR for the 2-leaf, the triangle and the quadrilateral together with our estimate \mathcal{L}_q given by (18). The former gives the number of active lengths and the latter an estimate of the sum of the lengths of the edges on which energy is concentrated.

	two leaf	triangle	quadrilateral
\mathcal{L}_q	1/2	1/3	1/4
IPR	$\frac{3}{2(l_1+l_2)}$	$\frac{3}{2(l_1+l_2+l_3)}$	$\frac{3}{2(l_1+l_2+l_3+l_4)}$

Table 7: Localization criterion \mathcal{L}_q and Inverse Participation Ratio (20) for three localized eigenvectors.

4.1 Exciting a localized eigenvector by a broadband pulse

An important practical issue is how to excite these localized eigenvectors. For the random fiber laser, the authors of [6, 7] send an electromagnetic pulse on a region of the network. They also couple the arcs on the boundary to an outside circuit to let energy escape. Then they expect that the only energy remaining will be that corresponding to the localized eigenvectors.

This argument is correct in principle. To confirm it, consider the eigenvectors shown in Fig. 3. All localized modes are away from the vertex 6 so the components at that vertex are exponentially small. Assume a Sommerfeld radiation condition at that vertex,

$$\epsilon U_t = U_x. \quad (21)$$

Then the boundary condition there becomes

$$\epsilon V_{j_x} + ikV_j = 0,$$

which is easily satisfied if $V_{j_x} = V_j = 0$. This simple argument shows that localized eigenvectors inside the graph will be preserved when the boundaries of the network are coupled to a dissipation source.

We illustrate this numerically on the G14 metric graph, using the finite difference code studied in the article [18]. We formed a localized eigenvector on the triangle defined by the arcs 1,3 and 5 for the 18th eigenvalue corresponding to $k = 1.133761002$. For that we chose the lengths of the arcs 1,3 and 5,

$$l_1 = \frac{4\pi}{k} \approx 11.451671, \quad l_3 = l_5 = \frac{2\pi}{k} \approx 5.909775.$$

Vertex 6 has a transparent boundary condition (21) ($\epsilon = 1$). The other external vertices have Neuman boundary conditions. We solve the generalized wave equation using the numerical procedure detailed in [18] and plot in Fig. 13 two snapshots of the time evolution of the components $U_j(x, t)$ on each arc j . At time $t = 0$, U is a gaussian on edge 5 and zero everywhere else, with 1 as initial velocity. The left panel shows a short time $t = 7 \cdot 10^4$ and the middle panel a much longer time $t = 4 \cdot 10^6$. For the former, the solution is still in a transient state while the latter indicates that we reached an asymptotic state corresponding to the localized eigenvector on the triangle 1-3-5. There the maximum of the solution is $2 \cdot 10^{-2}$ while it is $3 \cdot 10^{-3}$ on the other arcs. The histogram of the energies shown in the right panel of Fig. 13 shows that the energy is concentrated on the arcs 1-3-5. The energy of E_{13} is due to the large length of that arc $l_{13} = 22$.

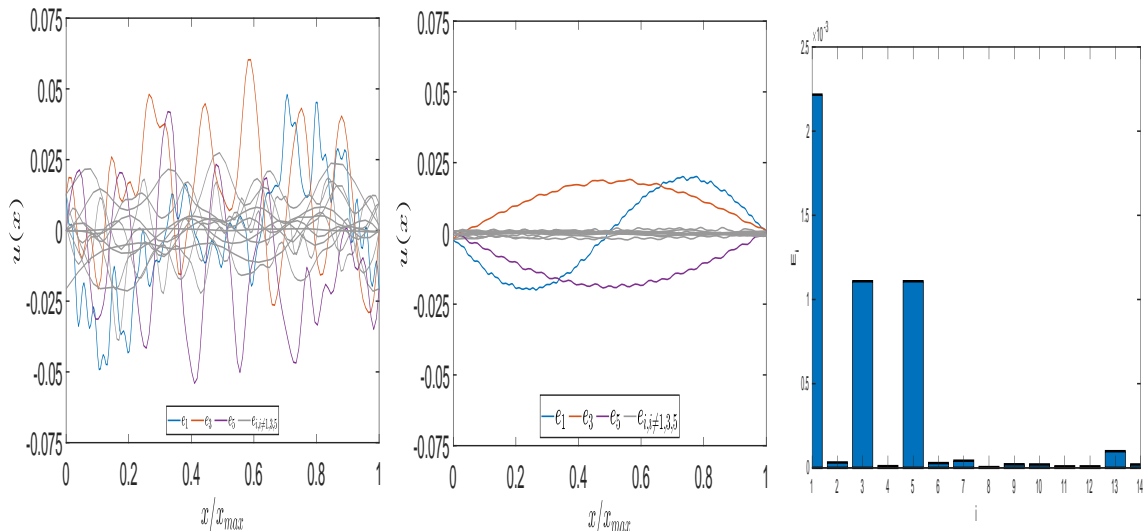


Figure 13: Numerical solution of the wave equation on the G14 metric graph for a broadband initial condition and a transparent boundary condition (21) at vertex 6. The left and middle panels show snapshots of the solution components $U_j(x, t)$ on each arc j for respectively $t = 7 \cdot 10^4$ and $t = 4 \cdot 10^6$. The right panel shows a histogram of the energies E_j on each edge j .

5 Conclusion

In this article we applied our algorithm to study the eigenvectors of two metric graphs arising in the modeling of the electrical grid and in a model of a random laser. We find that localized eigenvectors occur rarely and that the network needs to be tuned specifically for this.

We describe precise resonance conditions on the lengths of the arcs to obtain exactly localized eigenvectors. Some of these results were known, new results are the 1-2 arc cycle eigenvector in a pumpkin and the connection of localized eigenvectors to form a larger localized eigenvector.

We define a new localization criterion based on the L_2 norm which gives the number of active edges in an eigenvector, this quantity cannot be obtained from the standard IPR criterion. An important question is how to excite these localized eigenvectors? To answer this we showed, using the time dependent wave equation with a leaky boundary, that a localized eigenvector gets naturally excited in the long term from a broadband initial condition.

For the electrical grid application, even approximately localized eigenvectors can damage equipment so it should be reinforced in the regions of maximal amplitude of these localized eigenvectors. For a laser, a random arrangement

of wave guides graph will not in general lead to a lasing phenomenon. A laser should be built by associating structures corresponding to localized eigenvectors, not random links.

In the future, we plan to extend this study to nonlinear effects and examine the stability of the resonance to perturbations (quality factor). We will also examine non-Kirchhoff coupling conditions.

Acknowledgements

JGC thanks the Mathematics Department at the University of Arizona for its hospitality during the spring semesters 2022 and 2023. He is grateful to the Gaspard Monge foundation for support. HK thanks the ARCS Foundation for support.

References

- [1] M. Herty, J. Mohring and V. Sachers . A new model for gas flow in pipe networks. *Mathematical Methods in the Applied Sciences*, 33(7), 845-855, (2010).
- [2] A. Martin, K. Klamroth, J. Lang, G. Leugering, A. Morsi, M. Oberlack and R. Rosen, R. (Eds.), *Mathematical optimization of water networks* Vol. 162, Springer Science & Business Media, (2012).
- [3] P. Kundur, *Power System Stability and Control*, 1. New York: McGraw-Hill, (1994)
- [4] D. B. Work, and A. M. Bayen, . Convex formulations of air traffic flow optimization problems. *Proceedings of the IEEE*, 96(12), 2096-2112, (2008).
- [5] Z. Fu, T. Koch, T. M. Antonsen, E. Ott, and S. M. Anlage, Experimental Study of Quantum Graphs with Simple Microwave Networks: Non-Universal Features. *Acta Physica Polonica, A.*, 132(6), (2017)
- [6] M. Gaio, D. Saxena, J. Bertolotti, D. Pisignano, A. Camposeo, and R. Sapienza, . A nanophotonic laser on a graph. *Nature communications*, 10(1), 1-7, (2019).
- [7] O. Cipolato, Mode controllability of a Network Random Laser, Master thesis, University of Padova, (2020).
- [8] G. Berkolaiko, and P. Kuchment, *Introduction to quantum graphs* (No. 186). American Mathematical Soc., (2013).

- [9] J.-G. Caputo, A. Knippel, and E. Simo, . Oscillations of networks: the role of soft nodes. *Journal of Physics A: Mathematical and Theoretical*, 46(3), 035101, (2012).
- [10] J.-G. Caputo, G. Cruz-Pacheco, A. Knippel and P. Panayotaros, Spectra of chains connected to complete graphs. *Linear Algebra and its Applications*, 605, 29-62, (2020).
- [11] S. Hata, and H. Nakao, Localization of Laplacian eigenvectors on random networks. *Scientific reports*, 7(1), 1-11, (2017).
- [12] P. W. Anderson, . Absence of diffusion in certain random lattices. *Physical review*, 109(5), 1492, (1958)
- [13] F. Slanina, . Localization of eigenvectors in random graphs. *The European Physical Journal B*, 85(11), 1-12, (2012).
- [14] R. J. Bell, and P. Dean, Atomic vibrations in vitreous silica. *Discussions of the Faraday society*, 50, 55-61, (1970).
- [15] F. Klopp and K. Pankrashkin, . Localization on quantum graphs with random vertex couplings. *Journal of Statistical Physics*, 131(4), 651-673, (2008).
- [16] F. Klopp and K. Pankrashkin, . Localization on quantum graphs with random edge lengths. *Letters in Mathematical Physics*, 87(1), 99-114, (2009).
- [17] P. D. Hislop and O. Post, Anderson localization for radial tree-like random quantum graphs. *Waves in Random and Complex Media*, 19(2), 216-261, (2009).
- [18] M. Brio, J.-G. Caputo, and H. Kravitz, Spectral solutions of PDEs on networks. *Applied Numerical Mathematics*, 172, 99-117, (2022).
- [19] G. Berkolaiko, . An elementary introduction to quantum graphs. *Geometric and computational spectral theory*, 700, 41-72, (2017).
- [20] G. Berkolaiko, J. B. Kennedy, P. Kurasov, and D. Mugnolo, . Edge connectivity and the spectral gap of combinatorial and quantum graphs. *Journal of Physics A: Mathematical and Theoretical*, 50(36), 365201, (2017).
- [21] University of Illinois Information Trust Institute (2022), IEEE 14-Bus System, University of Illinois Board of Trustees, <https://icseg.itl.illinois.edu/ieee-14-bus-system/>.
- [22] S. Gnutzmann, H. Schanz, and U. Smilansky, Topological Resonances in Scattering on Networks (Graphs), *Phys. Rev. Lett.* 110, 094101, (2013).
- [23] H. Schanz and T. Kottos, Scars on Quantum Networks Ignore the Lyapunov Exponent *Phys. Rev. Lett.* 90, 234101, (2003).

A Exactly localized eigenvectors

A.1 Two connected leafs

Two connected leaves form the structure shown in Fig. 14.

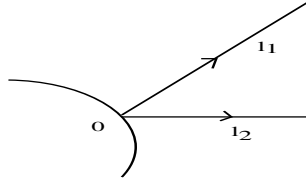


Figure 14: Two connected leaves in a graph.

Theorem A.1 *A localized eigenvector of the generalized Laplacian exists on two connected leaves of lengths l_1, l_2 if there exists two integers p, q such that*

$$(2p + 1)l_1 - (2q + 1)l_2 = 0.$$

Proof. An eigenvector localized on the two leaves satisfies the following conditions on the two eigenvector components,

$$V_i = A_i \sin kx + B_i \cos kx, \quad i = 1, 2$$

$$\begin{aligned} V_1(0) &= V_2(0) = 0, \\ V_{1x}(0) + V_{2x}(0) &= 0, \\ V_{1x}(l_1) &= 0, \\ V_{2x}(l_2) &= 0, \end{aligned}$$

From this system of equations we get

$$\begin{aligned} B_1 &= B_2 = 0, \\ A_1 + A_2 &= 0, \\ \cos kl_1 &= 0, \\ \cos kl_2 &= 0, \end{aligned}$$

so that

$$kl_1 = (2p + 1)\frac{\pi}{2}, \quad kl_2 = (2q + 1)\frac{\pi}{2}$$

These conditions are satisfied if l_1, l_2 verify

$$(2p + 1)l_1 - (2q + 1)l_2 = 0$$

where p, q are integers. □

Exactly localized eigenvectors also exist when there are three or more leaves. We sketch the situation for three leaves and give the result for L leaves. Assume there are three leaves. The conditions are then

$$B_1 = B_2 = B_3 = 0, \quad A_1 + A_2 + A_3 = 0, \\ \cos kl_1 = \cos kl_2 = \cos kl_3 = 0.$$

From this system we obtain the constraints on the lengths

$$(2p_1 + 1)l_1 - (2q_1 + 1)l_2 = 0, \\ (2p_2 + 1)l_1 - (2q_2 + 1)l_3 = 0, \\ (2p_3 + 1)l_2 - (2q_3 + 1)l_3 = 0,$$

where $p_1, p_2, p_3, q_1, q_2, q_3$ are integers. Note that the eigenspace has dimension 2.

For L connected leaves, we would get an eigenspace of dimension $L - 1$ and C_L^2 constraints defining k .

B Configurations with no exactly localized eigenvectors

B.1 No leaf localized eigenvector

A leaf is an arc such that its end vertex has degree 1, see Fig. 15.

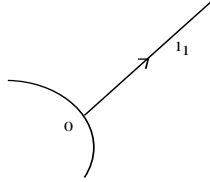


Figure 15: A leaf in a graph.

Theorem B.1 *There are no localized eigenvectors on leaves of a metric graph.*

Proof. Assume a leaf of length l , parameterized by $x \in [0, l]$. The boundary conditions at $x = 0, l$ are $V(0) = 0$, $V_x(0) = V_x(l) = 0$. Writing V as

$$V = A \sin kx + B \cos kx,$$

where all indices have been dropped for simplicity, we get from the first two conditions

$$A = B = 0,$$

so there are no eigenvectors localized on a leaf. □

B.2 No localized eigenvector on two connected arcs

We prove that no localized eigenvector exists on two arcs connected at one vertex, see Fig. 16.

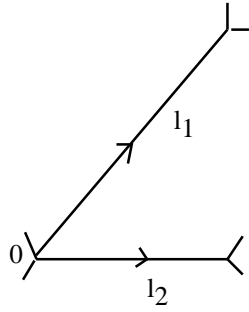


Figure 16: Two connected arcs "embedded" in a graph.

Theorem B.2 *A localized state cannot exist on two arcs connected at one vertex.*

Proof. The localization conditions for the eigenvector components are

$$\begin{aligned} V_1(0) &= V_2(0) = 0, \\ V_1(l_1) &= V_2(l_2) = 0, \\ V_{1x}(0) + V_{2x}(0) &= 0, \\ V_{1x}(l_1) + V_{2x}(l_2) &= 0, \end{aligned}$$

which yield the following system

$$\begin{aligned} B_1 &= B_2 = 0 \\ A_1 s_1 &= 0 \\ A_2 s_2 &= 0 \\ A_1 c_1 + A_2 c_2 &= 0 \\ A_1 c_1 &= 0 \\ A_2 c_2 &= 0, \end{aligned}$$

which only has the solution $A_1 = A_2 = 0$, so a localized eigenvector cannot exist. □

B.3 No degree three vertex eigenvector

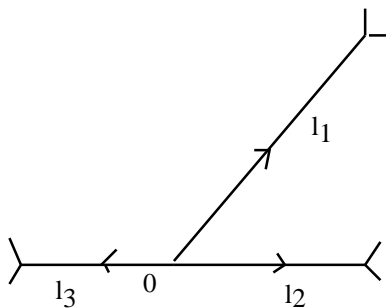


Figure 17: A degree three vertex "embedded" in a graph.

Consider the configuration of Fig. 17 where a degree three vertex is embedded in a graph, we have the following theorem.

Theorem B.3 *No eigenvector can be localized on three arcs connected at a single vertex.*

Proof. Let us write the components of an eigenvector localized on the subgraph l_1, l_2, l_3 . The conditions are

$$\begin{aligned} V_1(l_1) &= V_2(l_2) = V_3(l_3) = 0, \\ V_{1x}(l_1) &= V_{2x}(l_2) = V_{3x}(l_3) = 0, \\ V_{1x}(0) + V_{2x}(0) + V_{3x}(0) &= 0, \end{aligned}$$

yielding

$$\begin{aligned} A_1 + A_2 + A_3 &= 0, \\ A_1 c_1 - B_1 s_1 &= 0, \\ A_2 c_2 - B_2 s_2 &= 0, \\ A_3 c_3 - B_3 s_3 &= 0, \\ A_1 s_1 + B_1 c_1 &= 0, \\ A_2 s_2 + B_2 c_2 &= 0, \\ A_3 s_3 + B_3 c_3 &= 0, \end{aligned}$$

leading to the homogeneous linear system.

$$\begin{pmatrix} 1 & \cdot & 1 & \cdot & 1 & \cdot \\ c_1 & -s_1 & \cdot & \cdot & \cdot & \cdot \\ s_1 & c_1 & \cdot & \cdot & \cdot & \cdot \\ \cdot & \cdot & c_2 & -s_2 & \cdot & \cdot \\ \cdot & \cdot & s_2 & c_2 & \cdot & \cdot \\ \cdot & \cdot & \cdot & \cdot & c_3 & -s_3 \\ \cdot & \cdot & \cdot & \cdot & s_3 & c_3 \end{pmatrix} \begin{pmatrix} A_1 \\ B_1 \\ A_2 \\ B_2 \\ A_3 \\ B_3 \end{pmatrix} = \begin{pmatrix} 0 \\ 0 \\ 0 \\ 0 \\ 0 \\ 0 \end{pmatrix} \quad (22)$$

The determinant of the submatrix obtained by taking out the first line is equal to 1, so that the whole matrix has rank greater or equal to 6. Then there is no other solution than $A_1 = B_1 = A_2 = B_2 = A_3 = B_3 = 0$. \square